STRUCTURAL BIOLOGY
COMMUNICATIONS

Volume 71 (2015)

Supporting information for article:

Crystallographic insights into the structure–activity relationships of diazaborine enoyl-ACP reductase inhibitors

Cheryl A. Jordan, Braddock A. Sandoval, Mkrtich V. Serobyan, Damian H. Gilling, Michael P. Groziak, H. Howard Xu and Jessica L. Vey

Supporting information

Table S1 Macromolecule production information

Source organism	*Escherichia coli* strain MG1655
DNA source	*Escherichia coli* genomic DNA
Cloning vector	pET30 EK/LIC
Expression vector	pET30-ecFabI
Expression host	*Escherichia coli* BL21(DE3)
Complete amino acid sequence of the construct produced	MHHHHHHSSGLVPRGSGMKETAAAKFERQHMDSPDLGTDDDD KMGFLSGKRILVTGVASKLSIAYGIAQAMHREGAELAFTYQNDK LKGRVEEFAAQLGSDIVLQCDVAEDASIDTMFAELGKVWPKFDG FVHSIGFAPGDQLDGDYVNAVTREGFKIAHDISSYSFVAMAKACR SMLNPGSALLTLSYLGAERAIPNYNVMGLAKASLEANVRYMAN AMGPEGVRVNAISAGPIRTLAASGIKDFRKMLAHCEAVTPIRRTV TIEDVGNSAAFLCSDLSAGISGEVVHVDGGFSIAAMNELELK
Molecular Weight	32650.1 Da
Biological Functional Unit	Tetramer

Table S2 Crystallization

Method	Vapor diffusion
Plate type	Hanging drop
Temperature (K)	298
Protein concentration	10 mg/mL
Buffer composition of protein solution	20 mM tris pH 7.5, 1 mM DTT, 5% glycerol
Composition of crystallization solution	apo-FabI: 0.1*M* citrate pH 7.0, 0.1*M* ammonium sulfate, 22%*w*/*v* PEG 3350 14b-FabI: 0.1 M tris pH 8.5, 2.0 M ammonium sulfate 35b-FabI: 0.1 M HEPES pH 7.5, 2.0 M ammonium sulfate
Composition of reservoir solution	0.1*M* citrate pH 7.0, 0.1*M* ammonium sulfate, 22%*w*/*v* PEG 2000
Volume and ratio of drop	1 µL protein : 1 µL precipitant
Volume of reservoir	750µL

Table S3 Position of the disordered loop in each ecFabI chain.

Model	Chain A	Chain B
Apo-FabI	195 – 201	194 – 203
14b-FabI	195 – 203	195 – 202
35b-FabI	194 – 210	193 – 209

Figure S1 Representative FabI crystals. FabI crystallized in a hexagonal form in the presence and absence of inhibitors.

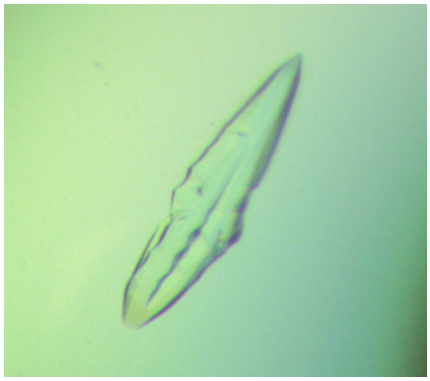

Figure S2 Representative FabI diffraction collected on beamline 12-2 at SSRL.

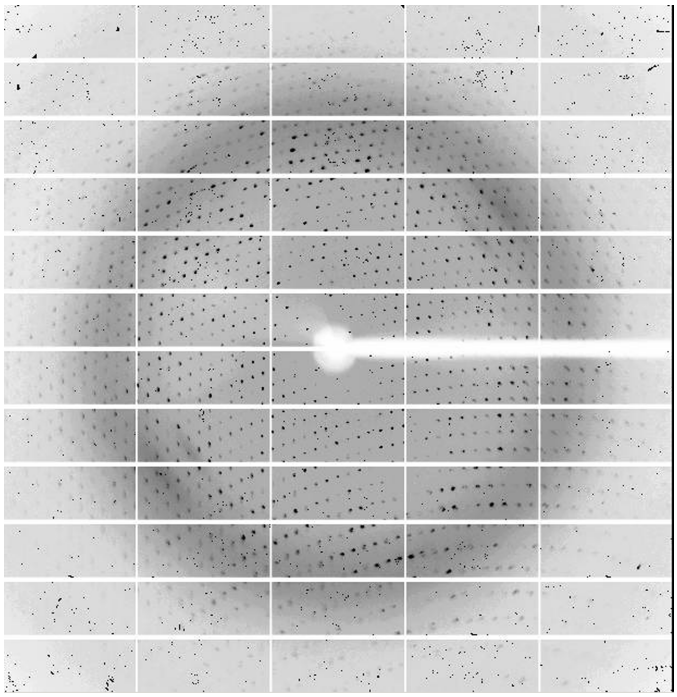

Figure S3 Stereoview of the ecFabI monomer. (a) Chain A of the ecFabI monomer is shown in cartoon representation as in Figure 3b with secondary structural elements labelled. The bound inhibitor-NAD^+ complex is shown in stick representation with NAD^+ carbons in yellow, inhibitor carbons in green, nitrogen atoms in blue, oxygen in red, and sulfur in gold.

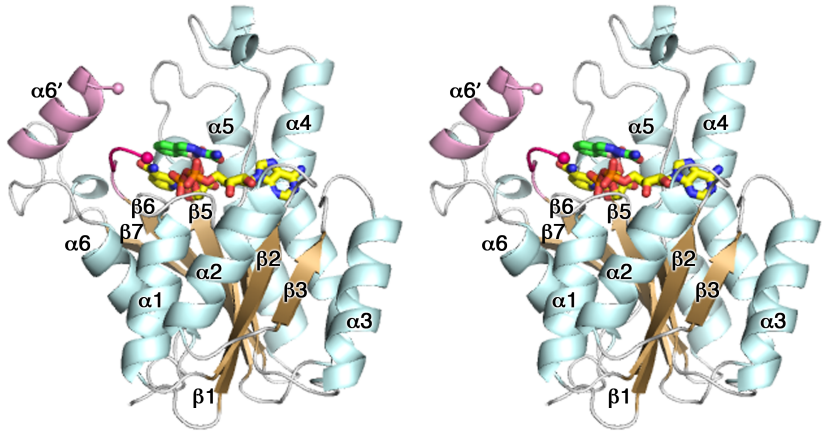

Figure S4 Comparison of diazaborine-bound and triclosan-bound FabI structures in the mobile active site loop region. Both models are shown in grey cartoons, with the exception of the flipping loop, which is colored blue in the triclosan-bound ecFabI model and magenta in the benzodiazaborine-bound ecFabI model. Bound molecules are shown in sticks colored as shown in previous figures (NAD, yellow carbons; triclosan, blue carbons; 2-tosyl-benzodiazaborine, magenta carbons). In (a), the two models are shown in the same orientation as Figure 6. In (b), the models are rotated 90° around an axis parallel to the plane of the paper.

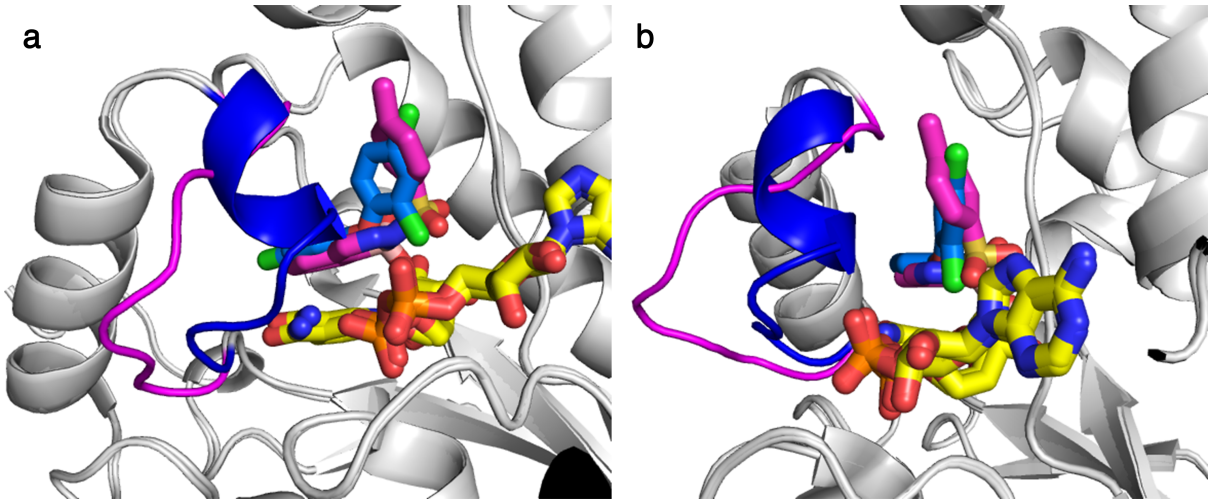

Figure S5 The flipping loop (residues 192-199) of 14b-FabI chain A. In the data reported here, very weak electron density is present where the loop would be expected. This density is generally consistent with a primarily disordered loop that approximates one of two previously observed conformations. (a) Superimposed 14b-FabI chains A and B are shown in white cartoons with the exception of the flipping loop, which is colored magenta (chain A) or yellow (chain B). The 14b-NAD^+ complex is shown in stick representation with dark grey carbons. (b) 14b-FabI chain A displayed as in (a) with the flipping loop shown in stick representation. $2F_o$-F_c density calculated from the 14b-FabI model with the flipping loop modelled and contoured at 1.0 σ around the entire flipping loop region (including the chain B orientation) is shown as a blue mesh. (c) F_o-F_c omit density calculated from the 14b-FabI model (with no flipping loop modelled) and contoured at 2.0 σ is shown as a cyan (positive difference density) or red (negative difference density) mesh. The omit map is shown covering the entire flipping loop region.

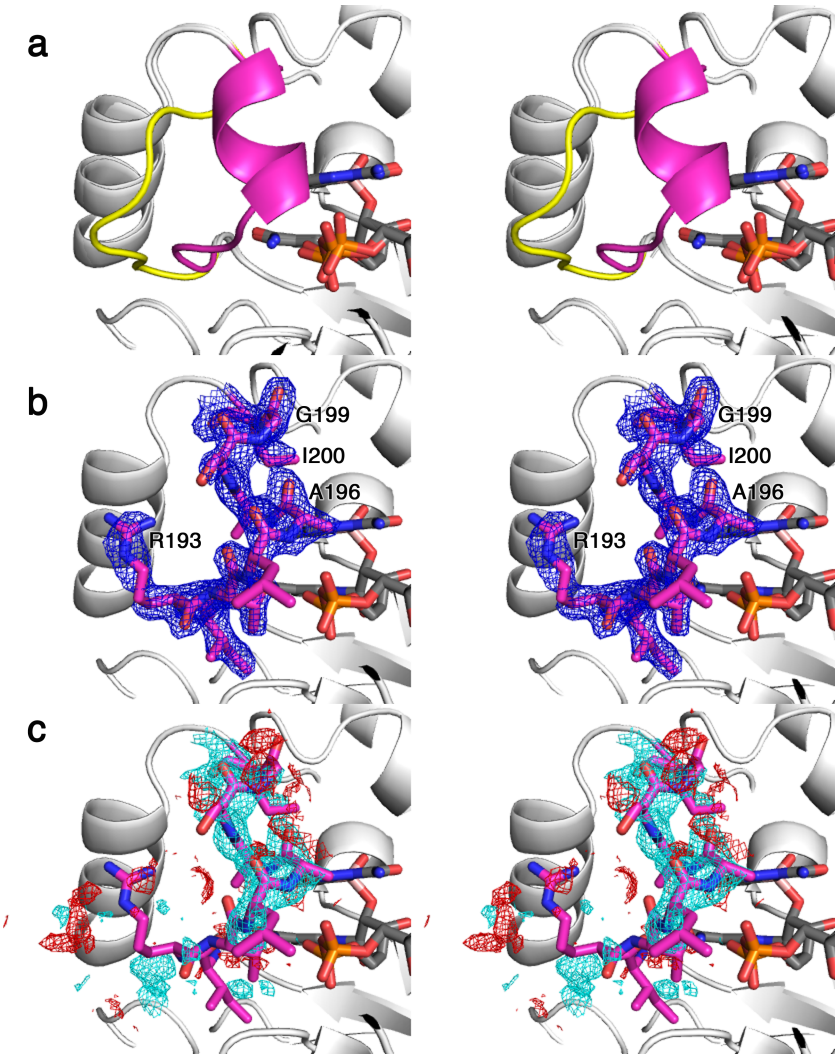

Figure S6 The flipping loop (residues 192-199) of 14b-FabI chain B. Parts (a) – (c) are shown as described in Figure S5, focusing here in parts (b) and (c) on chain B. The density in the area of this loop in chain B is significantly less intense than observed in the same region of chain A. Even so, the beginning of this loop (residues 192 – 194) clearly adopts an alternative conformation than observed in chain A.

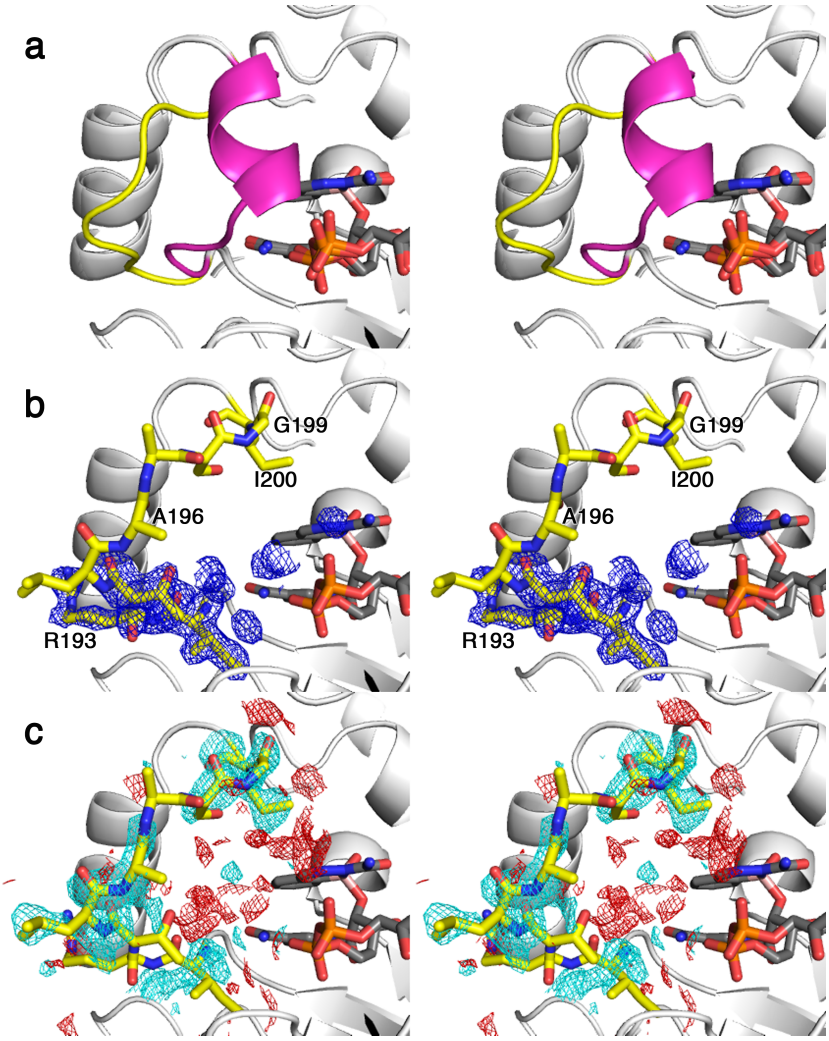

Figure S7 Comparison of the sulfonyl and (thio)carbonyl sidechain geometry. This figure is a stereoview of the 2-tosyl-benzodiazaborine-bound and 2-propylsulfonyl-thienodiazaborine-bound ecFabI structures (1dfg and 1dfh, respectively) shown superimposed upon the 14b-FabI structure (shown as white cartoons). The inhibitor binding site is shown with the NAD^+ omitted for clarity. 2-tosyl-benzodiazaborine and 2-propylsulfonyl-thienodiazaborine are shown in stick representation with magenta carbons, and molecule 14b is shown in sticks with green carbons.